McFarland, J. T., & Bernhard, S. A. (1972) *Biochemistry 11*, 1486–1493.
McIntyre, I. O., & Churchill, P. (1985) *Anal. Biochem. 147*, 468–477.
Ottolenghi, P., & Ellory, J. C. (1983) *J. Biol. Chem. 258*, 14895–14907.
Parkinson, D., & Callingham, B. A. (1982) *Radiat. Res. 90*, 252–259.
Reynolds, C. H., & McKinley-McKee, J. S. (1975) *Arch. Biochem. Biophys. 168*, 145–162.
Shikita, M., & Hatano-Sato, F. (1972) *FEBS Lett. 36*, 187–189.
Shore, J. D., & Theorell, H. (1966) *Arch. Biochem. Biophys. 117*, 375–380.
Suarez, M. D. (1986) Ph.D. Thesis, Michigan State University.
Turner, R. J., & Kempner, E. S. (1982) *J. Biol. Chem. 257*, 10794–10797.
Twu, J., Chin, C. C. Q., & Wold, F. (1973) *Biochemistry 12*, 2856–2862.
Vallee, B. L., & Hoch, F. L. (1955) *Proc. Natl. Acad. Sci. U.S.A. 41*, 327–338.
Venter, J. C. (1983) *J. Biol. Chem. 258*, 4842–4848.
Venter, J. C., Fraser, C. M., Schaber, J. S., Jung, C. Y., Bolger, G., & Triggle, D. J. (1983) *J. Biol. Chem. 258*, 9344–9348.
Wilkinson, G. N. (1961) *Biochem. J. 80*, 324–332.
Wills, C., & Jornvall, H. (1979) *Eur. J. Biochem. 99*, 323–331.

Optically Detected Magnetic Resonance of Tryptophan Residues in Complexes Formed between a Bacterial Single-Stranded DNA Binding Protein and Heavy Atom Modified Poly(uridylic acid)†

Mustafa I. Khamis, Jose R. Casas-Finet, and August H. Maki*
Chemistry Department, University of California, Davis, California 95616
Peter P. Ruvolo and John W. Chase
Department of Molecular Biology, Albert Einstein College of Medicine, Bronx, New York 10461
Received September 19, 1986; Revised Manuscript Received December 12, 1986

ABSTRACT: Optically detected magnetic resonance (ODMR) methods were employed to study three single-stranded DNA binding (SSB) proteins encoded by plasmids of enteric bacteria: pIP71a, R64, and F. Equilibrium binding isotherms obtained by fluorescence titrations reveal that the complexes of the plasmid SSB proteins with heavy atom modified polynucleotides are readily disrupted by salt. Since all the plasmid SSB proteins show limited solubility at low ionic strength (pIP71a > R64 > F), we were able to bind only the pIP71a protein to mercurated poly(uridylic acid) [poly(5-HgU)] and brominated poly(uridylic acid) [poly(5-BrU)]. ODMR results reveal the existence of at least one heavy atom perturbed, red-shifted, stacked Trp residue in these complexes. Amplitude-modulated phosphorescence microwave double resonance spectra display selectively the phosphorescence associated with Hg-perturbed Trp residue(s) in the pIP71a SSB protein–poly(5-HgU) complex, which has a broad, red-shifted 0,0-band. Our results suggest that Trp-135 in *Escherichia coli* SSB, which is absent in the plasmid-encoded SSB proteins, is located in a polar environment and is not involved in stacking interactions with the nucleotide bases. Phosphorescence spectra and lifetime measurements of the pIP71a SSB protein–poly(5-BrU) complex show that at least one Trp residue in the complex does not undergo stacking. This sets a higher limit of two stacking interactions of Trp residues with nucleotide bases in complexes of pIP71a SSB with single-stranded polynucleotides.

Single-stranded DNA (ssDNA)[1] binding proteins (SSB proteins) play a vital role in cellular processes such as DNA replication, recombination, and repair. SSB proteins that bind preferentially to single-stranded DNA and seem devoid of catalytic activity have been isolated from a variety of sources and organisms, both prokaryotic and eukaryotic. The physiological functions of these proteins have been best characterized from phage T4 and *Escherichia coli* [for reviews, see Falaschi et al. (1980), Kowalczykowsky et al. (1981), Williams and Konigsberg (1981), Hélène et al. (1982), and Chase and Williams (1986)]. Genetic analysis of conditional lethal mutants of *E. coli* single-strand binding protein (Eco SSB) has established its necessary role in DNA replication, repair, and recombination (Meyer et al., 1979; Whittier & Chase,

†This research was supported by National Institutes of Health Grants ES02661 (A.H.M.) and GM11301 and CA13330 (J.W.C.). M.I.K. is grateful for fellowship support from Amideast.
* Correspondence should be addressed to this author.

[1] Abbreviations: AM-PMDR, amplitude-modulated phosphorescence microwave double resonance; D and E, triplet-state zero-field splitting parameters; dsDNA, double-stranded DNA; EDTA, ethylenediaminetetraacetic acid; Lys-Trp-Lys, lysyltryptophyl-α-lysine; ODMR, optically detected magnetic resonance; pIP71a SSB, single-stranded DNA binding protein encoded by pIP71a, an Inc9 plasmid; pIP231a SSB, single-stranded DNA binding protein encoded by pIP231a, an IncY plasmid; R64 SSB, single-stranded DNA binding protein encoded by R64, an $IncI_1$ plasmid; *E. coli* SSB (*Eco* SSB), single-stranded DNA binding protein encoded by *Escherichia coli*; F plasmid SSB (F SSB), *E. coli* F plasmid encoded single-stranded binding protein; poly(dT), poly(deoxythymidylic acid); poly(5-BrU), brominated poly(uridylic acid); poly(5-HgU), mercurated poly(uridylic acid); ssDNA, single-stranded (heat-denatured) DNA; Trp, tryptophan.

0006-2960/87/0426-3347$01.50/0

1983; Lieberman & Witkin, 1983; Golub & Low, 1983; Chase et al., 1984). Two of these mutant SSB proteins, SSB-1 and SSB-113, have been well studied, both from the genetic and physicochemical point of view [for a review, see Chase (1984) and references cited therein]. It has been shown that the conjugative plasmid F of *E. coli*, which codes for its own single-stranded DNA binding protein (F SSB), can partially complement the *ssb-1* defect in the chromosomal SSB (Kolodkin et al., 1983). F SSB protein presents extensive sequence homology to *E. coli* SSB (Chase et al., 1983). Recently, Golub and Low (1985) have obtained evidence that other transmissible plasmids encode SSB-like proteins and have cloned the genes that are responsible for the complementation of the *ssb-1* defect from conjugative plasmids belonging to three different incompatibility (Inc) groups. The analysis of F SSB protein as well as analogous proteins from these other plasmids may help us to understand the relationship between structure and function for these systems. We focus in this paper on the results of a study by optically detected magnetic resonance (ODMR) spectroscopy on the pIP71a (an Inc9 plasmid) encoded SSB protein and its complexes with heavy atom modified polynucleotides.

The SSB proteins encoded by enteric bacterial plasmid pIP71a, pIP231a, and R64 share extensive sequence homology with *Eco* SSB and even greater homology with F SSB (P. Ruvolo and J. Chase, unpublished results; Sancar et al., 1981; Chase et al., 1983). The most extensive sequence homology occurs within the NH_2-terminal regions. For example, 85 of the first 115 amino acid residues of F SSB are identical with those of *Eco* SSB, and 112 of the first 115 amino acid residues of pIP71a SSB are identical with those of F SSB. The significance of this extreme conservation of sequence (and perhaps structure) may be explained by the demonstration from analysis of partial proteolysis products of *Eco* SSB that the DNA binding region is contained in the NH_2-terminal region (Williams et al., 1981). The sequences of these proteins diverge extensively in the COOH-terminal regions, although small areas of homology exist. One of the four tryptophan residues of *Eco* SSB, located in the COOH-terminal region, is missing in each of the plasmid-encoded SSB proteins mentioned above. It has been proposed that aromatic residues are involved in the binding of oligopeptides (Hélène & Maurizot, 1981) and proteins (Köster, 1980) to single-stranded polynucleotides. Stacking interactions of Trp residues of *Eco* SSB with nucleic acids have been reported (Cha & Maki, 1984b; Khamis et al., 1987). Removal of a 7-kDa fragment (including Trp-135) from the carboxy terminus of *Eco* SSB results in a partial proteolysis product that actually binds 3 times more tightly than does the intact protein to single-stranded DNA (Williams et al., 1983). Thus, it seems unlikely that Trp-135 is involved in the protein binding, leaving Trp-40, -54, and -88 as candidates for involvement in stacking interactions with the polynucleotide bases (Khamis et al., 1987). The SSB protein encoded by pIP71a contains these three Trp residues at positions homologous to those in *Eco* SSB. Hence, it constitutes a simpler system than *Eco* SSB, to which ODMR spectroscopy can be applied to obtain detailed information on the triplet-state properties of its Trp residues. When used in conjunction with the external heavy atom effect (Kasha, 1952), ODMR is able to determine the occurrence of close-range interactions between Trp and heavy atom containing perturbers in biologically important protein–nucleic acid complexes (Cha & Maki, 1984b; Khamis & Maki, 1986; Khamis et al., 1987). Significant heavy atom effects are expected only if the perturber atom and the perturbed molecule are in van der Waals contact. We present evidence in this study for the involvement of at least one of the Trp residues of pIP71a SSB protein in stacking interactions with nucleotide bases, upon binding to mercurated poly(uridylic acid) [poly(5-HgU)]. Our measurements also support previous evidence (Williams et al., 1983) that Trp-135 is not directly involved in the binding process and, furthermore, is subject to polar interactions (Khamis et al., 1987). A bromine-modified polynucleotide [poly(5-BrU)] is introduced as another heavy atom derivatized ligand, and the effects produced by the two perturbing external heavy atoms, bromine and mercury, are compared. Fluorescence binding isotherms for the binding of pIP71a SSB to various synthetic homopolymers and single-stranded and double-stranded DNA also are provided. Our results show significant analogies between pIP71a SSB and *Eco* SSB binding to polynucleotides, as well as some differences. Other studies on the SSB proteins from plasmids F and R64 are currently in progress and may improve our general understanding of the function of these types of proteins.

Materials and Methods

The SSB proteins used in this study were prepared by using either published procedures (Chase et al., 1980, 1984) or slight modifications of these procedures (P. Ruvolo and J. Chase, unpublished results). Details of the cloning of the genes encoding pIP71a SSB, pIP231a SSB, and R64 SSB, their expression in *E. coli*, and the purification of the proteins will be described elsewhere.

The concentration of the pIP71a, F, and R64 single-stranded DNA binding proteins was determined by amino acid analysis. Poly(5-HgU) was obtained from P-L Biochemicals and was used without further purification. According to the manufacturer, greater than 70% of the uridine bases in the poly(5-HgU) supplied are mercurated covalently at the 5-position. Poly(5-BrU) was prepared by reaction of bromine with poly(U) in a modification of the procedure used to prepare poly(5-BrC) (Deubel & Leng, 1974) as described previously (Khamis & Maki, 1986). The concentrations of the polynucleotide samples were determined spectrophotometrically by using the following extinction coefficients (per mole of nucleotide): poly(5-HgU), $\epsilon_{267} = 1.5 \times 10^4$ M^{-1} cm^{-1}; poly(5-BrU), $\epsilon_{278} = 6.9 \times 10^3$ M^{-1} cm^{-1} (Michelson et al., 1962). Stock solutions of poly(5-HgU) and poly(5-BrU) were prepared by dissolving the polynucleotide in 1 mM cacodylate buffer (pH 7.0) containing 0.1 mM EDTA. All other chemicals were of the highest available purity.

Protein complexes were prepared by mixing appropriate volumes of stock solutions with the sample buffer and were incubated at 37 °C for 10 min. The composition of the sample buffer was 20 mM cacodylate (pH 7.0), 5 mM 2-mercaptoethanol, 0.1 mM EDTA, and 0.3 M NaCl in order to provide high ionic strength to prevent protein precipitation (vide infra). The excess of 2-mercaptoethanol relative to Hg present in the pIP71a SSB protein–poly(5-HgU) complex served as blocking reagent for Hg (Cha & Maki, 1982). A 30% (v/v) concentration of glycerol was maintained in the samples and served as cryogenic solvent for low-temperature work. Fifteen-microliter samples were transferred to a Suprasil quartz sample tube (1-mm inner diameter) which was then placed within a microwave helix terminating a coaxial transmission line and immersed in liquid nitrogen or liquid helium for spectroscopic measurements.

The apparatus and experimental procedures for measurements of phosphorescence spectra, lifetimes, and ODMR responses have been described previously (Maki & Co, 1976; Cha & Maki, 1982, 1984a,b; Ghosh et al., 1984). We will

present briefly the techniques employed for the present work.

Usually, before any ODMR measurements were performed, the phosphorescence spectrum and decay were measured so that the emission wavelength to be monitored and the microwave sweep time for the subsequent ODMR experiments could be chosen. Phosphorescence spectra were taken by using a rotating can sector (dead time of ca. 800 μs) to eliminate fluorescence and scattered light. For decay measurements, the sample was excited for a period of ca. 5 times the longest observed exponential component so that the decay would occur from the photostationary state. The multiexponential decays were deconvoluted and analyzed by computer as described earlier (Maki & Co, 1976; Khamis et al., 1987).

All ODMR measurements were performed in zero magnetic field and at pumped liquid helium temperature (ca. 1.2 K) in order to quench the spin–lattice relaxation. The signals were electronically filtered and signal-averaged to improve the signal-to-noise ratio. Slow-passage ODMR is used for the accurate determination of resonance frequencies and line shapes. The experiment is performed with continuous optical pumping and involves the passage of microwaves through a zero-field transition in a time that is slow compared with the longest sublevel lifetime. Microwave frequencies that match the energy difference between sublevels induce magnetic resonance transitions which may be detected as an intensity change in the phosphorescence emission. Accurate transition frequencies were determined by calibration of microwave sweeps with a frequency counter, and rapid-passage effects were compensated by extrapolation of the peak frequency to zero sweep rate (Khamis et al., 1987).

A fast-passage transient ODMR experiment was performed in the same way as that of slow-passage ODMR, except that the microwaves were swept through a transition faster than the shorter lived sublevel decay time in the transition pair. In this way a biexponential transient response composed of the decays of the individual sublevels connected by the transition could be obtained (Winscom & Maki, 1971).

The experimental details of the AM-PMDR method (Olmsted & El-Sayed, 1974) as carried out in our laboratory have been reported elsewhere (Davis & Maki, 1982; Cha & Maki, 1984a,b). This method applies amplitude modulation (AM) to the microwave output fixed at a resonance frequency; lock-in detection performed by a phase-sensitive detector discriminates between the phosphorescence spectra of chromophores emitting in the same spectral region, provided the microwave frequency corresponds to an ODMR signal of only one of them. The AM-PMDR method is only feasible for short-lived triplet states whose phosphorescence intensity is capable of responding at a reasonable AM frequency.

Titrations monitoring the intrinsic Trp fluorescence of pIP71a SSB protein were performed in a Perkin-Elmer MPF-44B spectrofluorometer using a 150 W Xenon lamp; the instrument was equipped with a thermostated cuvette holder. Titrations were performed at 25 °C with 2.0 mL of ca. 3×10^{-7} M solution of pIP71a SSB protein in a Suprasil quartz fluorescence cell (Hellma, 1.0 × 1.0 cm), unless otherwise indicated. Initially, the solvent used for fluorescence titrations was 20 mM cacodylate buffer (pH 7.0) containing 150 mM NaCl and 0.1 mM EDTA, as was used in similar studies on *Eco* SSB (Khamis et al., 1987). Titrations performed under these conditions produced inconsistent results, however, characterized by an anomalously low value for the protein binding site (n, number of nucleotide bases covered per protein molecule). At the pIP71a SSB concentrations used for our fluorometric titrations ($<10^{-6}$ M) some precipitation of the protein occured at [NaCl] <0.3 M. Addition of 10% glycerol to the buffer prevented protein precipitation at [NaCl] = 0.2 M; stoichiometric pIP71a SSB–polynucleotide complexes were stable at [NaCl] <0.15 M. pIP71a SSB precipitation also depended on the protein concentration. Addition of NaCl to pIP71a SSB samples prepared at low ionic strength results in an increase of their intrinsic tryptophan fluorescence emission. pIP71a SSB samples prepared in a 20 mM cacodylate buffer (pH 7.0) containing 10% glycerol, 5 mM 2-mercaptoethanol, 0.1 mM EDTA, and 0.3 M NaCl yielded consistent binding site size values that are comparable with those obtained for *Eco* SSB protein under conditions of high ionic strength (Lohman & Overman, 1985; Lohman et al., 1986). Ionic strength dependent precipitation of SSB proteins encoded by the *E. coli* plasmids F and R64 also occurred; an even higher NaCl concentration was required to avoid it (Casas-Finet, Khamis, Maki, and Chase, unpublished results).

Nucleic acid solutions were made in the same buffer as described above. Concentrations of solutions of poly(dT) and double-stranded calf thymus DNA were determined by ultraviolet absorbance, using the following extinction coefficients (in moles of phosphate residues): 8.52×10^3 M^{-1} cm^{-1} at 264 nm for poly(dT) (Ts'o et al., 1966) and 6.5×10^3 M^{-1} cm^{-1} at 260 nm for calf thymus dsDNA (McConnell & von Hippel, 1970). When necessary, DNA was denatured by boiling a 10^{-3} M solution in a sealed flask for 15 min. The boiling solution was rapidly cooled in an ice bath. The resulting hyperchromism was about 30%.

Aliquots of polynucleotides were added to the cell and were stirred with a Teflon-coated magnetic bar. Stepwise titration of fluorescence quenching was monitored at constant emission wavelength. The excitation wavelength was 282 nm with 2-nm slit width, and the emission wavelength was 345 nm with 6-nm slit width. Several fluorescence readings were accumulated with 5-s acquisition time and averaged. In order to minimize photobleaching of the Trp chromophores, the excitation shutter remained closed when data acquisition was not performed. Correction for the induced inner-filter effect was determined by parallel titrations of the model noncomplexing fluorophore *N*-acetyl-L-tryptophanamide (in solutions showing a total fluorescence emission equivalent to that of the pIP71a SSB protein) with the polynucleotide of interest. Salt back-titrations were performed by addition of aliquots of either a 5 M NaCl solution or a 3.5 M $MgCl_2$ solution. Analysis of the equilibrium binding isotherms was done as previously described (Williams et al., 1983).

Results and Discussion

Equilibrium Binding Isotherms of pIP71a SSB Complexed with Polynucleotides. *Eco* SSB exhibits an intrinsic fluorescence emission that is partially quenched upon nucleic acid binding (Molineux et al., 1975; Williams et al., 1983). As expected, the tryptophan fluorescence of pIP71a SSB also is quenched upon binding to nucleic acids. The fluorescence of pIP71a SSB was monitored as a function of the concentration of various polynucleotides, and the equilibrium binding isotherms were analyzed to calculate the magnitude of the association constant ($K\omega$) and maximum fluorescence quenching (Q_{max}). The maximum fluorescence quenching varies with the polynucleotide (Table I); it is the lowest for calf thymus dsDNA (0.23) and reached a limiting value of 0.88 of the pIP71a SSB intrinsic fluorescence emission when bound to ssDNA and poly(dT). These values are similar to those found in earlier studies of *Eco* SSB binding to poly(5-HgU) and poly(5-BrU) (0.46 and 0.88, respectively; Khamis et al., 1987) and to poly(dT) (0.80; Krauss et al., 1981). The

Table I: Determination of Binding Constants from Fluorescence Equilibrium Binding Isotherms for Complexes of pIP71a SSB Protein with Various Polynucleotides[a]

polynucleotide	$K\omega$ (M^{-1})	Q_{max}	salt-back midpoint (M)
poly(5-HgU)		0.48	0.34
poly(5-BrU)	2.1×10^8	0.88	0.98
poly(dT)	1.9×10^9	0.88	>3
calf thymus ssDNA	1.5×10^8	0.87	0.94
calf thymus dsDNA	7.4×10^4	0.23	0.90

[a] Fluorescence measurements are conducted as described under Materials and Methods. The pIP71a SSB protein concentration is 3.2×10^{-7} M. The buffer is 0.5 M in NaCl except for the titrations with poly(5-BrU) and poly(5-HgU), where the salt concentration is 0.4 and 0.15 M, respectively. Corrections are made for salt-dependent changes in protein intrinsic fluorescence.

ratio of the observed fluorescence quenching, at a given NaCl concentration, to the maximum fluorescence quenching (Q_{max}) reflects the fractional pIP71a SSB saturation, $(\text{pIP71a SSB})_{bound}/(\text{pIP71a SSB})_{total}$. Therefore, salt back-titrations (see Materials and Methods) allow us to estimate the resistance of the different complexes to disruption by NaCl. The salt-back midpoints found for the pIP71a SSB complexes (Table I) are of the same order as those of the *Eco* SSB complexes (Khamis et al., 1987). However, the limited solubility of the pIP71a SSB protein makes it difficult to accomplish saturation of the protein at the ionic strength needed to avoid precipitation. The pIP71a SSB–poly(dT) complex has a salt-back midpoint above 3 M NaCl, in accord with the finding that complexes of *Eco* SSB with poly(dT) do not dissociate in buffers containing as much as 5 M NaCl (Lohman & Overman, 1985).

Fluorescence quenching experiments provide only a lower limit for the affinity of pIP71a SSB for poly(dT) or ssDNA. As in the case of *Eco* SSB, pIP71a SSB protein has the highest affinity for binding to poly(dT) ($K\omega = 1.9 \times 10^9$ M^{-1}; see Table I). This value is in the range that was estimated for the affinity of *Eco* SSB for poly(dT) or ssDNA (10^8–10^{10} M^{-1}; Lohman & Overman, 1985; Molineux et al., 1975). The binding of pIP71a SSB to dsDNA is characterized by a low association constant which suggests noncooperative binding (Table I). Thus, comparison with the measured (cooperative) affinity of pIP71a SSB for ssDNA leads to an approximate value of about 10^3 for the cooperativity parameter (ω), which is close to that reported for the *Eco* SSB and phage T4 gene 32 proteins (Chase & Williams, 1986). A comparative study of the binding of the three plasmid-encoded SSB proteins pIP71a, R64, and F will be presented elsewhere.

Phosphorescence Spectra and Lifetime. (A) pIP71a SSB and Its Complex with Poly(5-HgU). The phosphorescence spectra of pIP71a SSB and the pIP71a SSB–poly(5-HgU) complex are shown as spectra A and B, respectively, of Figure

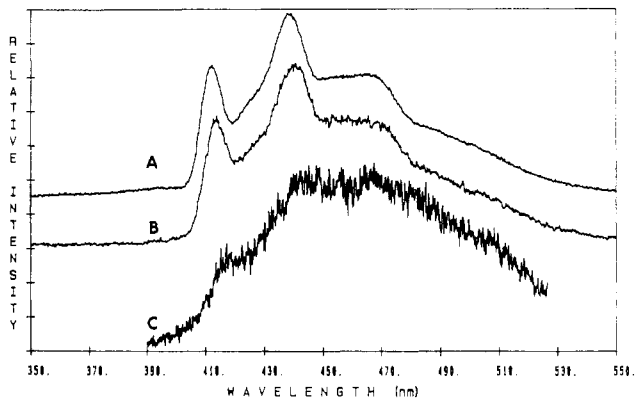

FIGURE 1: Phosphorescence spectra of (A) pIP71a SSB (8.6×10^{-5} M) and (B) pIP71a SSB (8.6×10^{-5} M) complexed with poly(5-HgU) (1.6×10^{-3} M) and (C) AM-PMDR spectrum of the pIP71a SSB–poly(5-HgU) complex. The AM-PMDR spectrum was obtained by amplitude modulation at 25 Hz of microwaves which were frequency modulated between 3.85 and 4.78 GHz at 3 KHz. Signal averaging was carried out for 10 wavelength scans. Spectra A and B are obtained at 4.2 K, while spectrum C is obtained at 1.2 K. Excitation is at 295 nm with 16-nm band-pass, and the emission slits are set at 3 nm.

1. The 0,0-band of Trp in pIP71a SSB (Figure 1A, Table II) is quite red shifted and peaks at 412.8 nm. The Trp 0,0-band λ_{max} of R64 SSB and F SSB are also presented for comparison in Table II. The λ_{max} of each SSB protein is red-shifted compared with that of the solvent-exposed Trp of Lys-Trp-Lys, which occurs at 409 nm. Comparison of the Trp 0,0-band of these three plasmid-encoded SSB proteins with that of *Eco* SSB (Table II) reveals that a consistent red shift of the 0,0-band is observed in the three plasmid proteins relative to that of *Eco* SSB. It is worth mentioning again that although these proteins show a high degree of homology of their amino acid sequences, Trp-135, located in the C-terminal region of *Eco* SSB, is absent in the plasmid SSB proteins (pIP71a, F, R64). These results suggest that Trp-135 is blue-shifted relative to the three other common Trp residues (Trp-40, Trp-54, and Trp-88). A blue-shifted 0,0-band is exhibited by Trp residues that are exposed to the solvent rather than buried in a hydrophobic region of the protein structure (Purkey & Galley, 1980), although Trp buried in a region undergoing polar interactions may also be blue-shifted (Hershberger et al., 1980). It is worth mentioning that two types of Trp sites have been characterized in *Eco* SSB, one of them more solvent exposed than the other (Khamis et al., 1987; Bandyopadhyay & Wu, 1978). On the basis of our present results we can assign Trp-135 to a blue-shifted site in *Eco* SSB.

When pIP71a SSB binds to poly(5-HgU) under conditions where 55% of the protein is in the bound state (since the limited solubility of the protein at lower ionic strength prevents us from obtaining a higher percentage of the complex), a

Table II: Tryptophan Zero-Field ODMR Frequencies and Zero-Field Splitting Parameters in Various Bacterial SSB Proteins and Complexes with Heavy Atom Modified Polynucleotides[a]

sample	$\lambda_{0,0}$ (nm)	$\lvert D\rvert - \lvert E\rvert$ (GHz)	$2\lvert E\rvert$ (GHz)	$\lvert D\rvert + \lvert E\rvert$ (GHz)	$\lvert D\rvert$ (GHz)	$\lvert E\rvert$ (GHz)
pIP71a SSB	412.8	1.734	2.555	–[b]	3.012	1.278
F SSB	412.8	1.739	2.532	–[b]	3.005	1.266
R64 SSB	412.2	1.722	2.546	–[b]	2.995	1.273
pIP71a SSB + poly(5-HgU)	413.6	1.807	2.670	4.432	3.142	1.335
pIP71a SSB + poly(5-BrU)	417.2	1.647	2.658	4.201	2.976	1.329
Eco SSB[c]	411.8	1.708	2.568	–[b]	2.992	1.284
Eco SSB + poly(5-HgU)[c]	413.6	1.780	2.551	4.346	3.063	1.276
Eco SSB + poly(5-BrU)[c]	415.2	1.655	2.610	4.275	2.965	1.305

[a] Measurements are made at 1.2 K with the monochromator at 3-nm resolution. Transition frequencies are corrected for rapid-passage effects. [b] Signal is not observed. [c] From Khamis et al. (1986).

Table III: Phosphorescence Lifetimes of Plasmid-Encoded SSB Proteins and of pIP71a SSB Complexes with Poly(5-HgU) and Poly(5-BrU)[a]

sample	λ_{em} (nm)	lifetime components[b]
pIP71a SSB	412.2	1.48 (15), 5.76 (85)
F SSB	413.0	2.58 (33), 6.10 (67)
R64 SSB	411.0	1.77 (13), 6.25 (87)
pIP71a SSB + poly(5-HgU)	413.4	0.70 (9), 6.12 (91)[c]
pIP71a SSB + poly(5-BrU)	417.0	0.50 (29), 5.50 (71)
pIP71a SSB + poly(5-BrU)[d]	417.0	0.58 (66), 4.33 (34)

[a] Measurements are made at 77 K, unless otherwise specified; the excitation wavelength is 295 nm, and the emission is monitored with 3-nm slit width. [b] Decay was fit to two exponential components with lifetimes as given (in units of seconds) and preexponential contributions as given in parentheses (in units of percent). [c] Also present was a short component of less than 10 ms, which was too short to analyze accurately. [d] Data obtained at 4.2 K.

broadened, red-shifted 0,0-band is observed (Figure 1B, Table II). Similar effects of poly(5-HgU) binding have been observed earlier in *Eco* SSB–poly(5-HgU) and gene 32 protein–poly(5-HgU) complexes (Khamis et al., 1987; Khamis & Maki, 1986). The limited solubility of F SSB and R64 SSB and the sensitivity of their complexes with poly(5-HgU) to disruption by high ionic strength (Casas-Finet, Khamis, Maki, Ruvolo, and Chase, unpublished results) ruled out similar experiments with these proteins.

The characteristics of the phosphorescence of the pIP71a SSB–poly(5-HgU) complex points to the contribution of perturbed Trp residues whose emission is shifted to the red. This conclusion is given support by the AM-PMDR spectrum (Figure 1C), which displays selectively the phosphorescence emission of the heavy atom perturbed Trp residues in the complex. Inspection of the AM–PMDR spectrum confirms that the 0,0-band of the heavy atom perturbed Trp residues is severely broadened and red-shifted (417 nm). Further discussion of this spectrum will be presented in a later section.

Lifetime measurements of the pIP71a SSB, F SSB, and R64 SSB proteins reveal the existence of normal Trp lifetimes with small contributions of Tyr residues (Table III). However, when pIP71a SSB complexes with poly(5-HgU), a very short lived (<10-ms) Trp component lifetime (too short to measure accurately) appears in the decay profile (Table III) and is indicative of an external heavy atom effect. It is noteworthy that 2-mercaptoethanol was added to the polynucleotide and served as a blocking reagent for the other valence of mercury. Due to steric considerations and the extremely close range requirement for an external heavy atom effect of this magnitude, we are led to the conclusion that stacking interactions between at least one Trp residue in the protein and the nucleotide bases are present. Due to the short lifetime requirements of the Trp site(s) producing the AM-PMDR spectrum (Figure 1C), it follows that these heavy atom perturbed Trp residues produce the observed AM-PMDR. The red shift of the phosphorescence also is consistent with stacking interactions (Rahn et al., 1966). Further evidence for this conclusion is provided in the ODMR section.

(B) pIP71a SSB–Poly(5-BrU) Complex. The phosphorescence spectrum of pIP71a SSB–poly(5-BrU) at 77 K is presented in Figure 2B. The 0,0-band peaks at 413.0 nm, is slightly red shifted compared with that of the protein itself (Figure 2A), and is broadened significantly. Furthermore, when the sample is cooled to 4.2 K, a more red shifted ($\lambda_{0,0} \sim 417.0$ nm), broad phosphorescence is obtained (Figure 2C). The features of this spectrum resemble to a great extent those of the Hg-perturbed Trp in pIP71a SSB–poly(5-HgU) complex, which were revealed by the AM-PMDR measurements

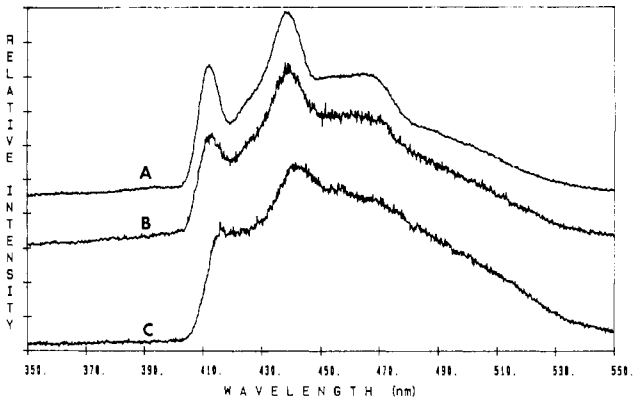

FIGURE 2: Phosphorescence spectra of (A) pIP71a SSB (8.6×10^{-5} M) and (B and C) pIP71a SSB (8.6×10^{-5} M) complexed with poly(5-BrU) (1.35×10^{-3} M). Excitation conditions are as given in Figure 1. (A) and (B) are at 77 K, and (C) is at 4.2 K.

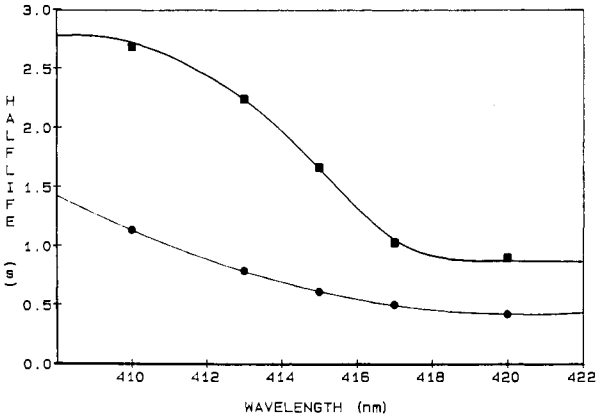

FIGURE 3: Plot of phosphorescence decay half-life vs. wavelength for the pIP71a SSB–poly(5-BrU) complex. Measurements are made at 77 K (filled squares) and 4.2 K (filled circles). Sample concentration and excitation conditions are as given in Figure 2.

(Figure 1C). A similar temperature dependence for Br atom perturbed Trp was observed earlier in the case of the *Eco* SSB–poly(5-BrU) complex (Khamis et al., 1987) as well as for the Lys-Trp-Lys–poly(dA-5BrdU) complex (Maki & Cha, 1984). This effect is probably due to the presence of stacked, red-shifted Trp residues which act as energy traps at 4.2 K.

Analysis of phosphorescence lifetimes of the pIP71a SSB–poly(5-BrU) complex reveals the existence of a readily measurable component with shorter decay lifetime (Table III). Furthermore, upon variation of the monitoring wavelength through the Trp 0,0-band to the red, an accompanying decrease in the phosphorescence *half-life* is observed (Figure 3). (The decay profile is in each case very complex; consequently, a multiexponential analysis was not attempted. A single half-life for the decay is reported, which reflects in a qualitative way the degree of short-component contribution to the decay.) It is noteworthy that the contribution of long-lived, and thus unperturbed, Trp to the decay is larger at 77 K than at 4.2 K, where the contribution of perturbed Trp residues is quite significant. Furthermore, the reduction of $t_{1/2}$ with increasing wavelength indicates that the heavy atom perturbation is accompanied by a red shift of the phosphorescence. These red-shifted sites appear to act as energy traps at 4.2 K and hence become dominant in the decay. Further evidence, provided by ODMR spectroscopy, for the presence of such perturbed Trp residue(s) in this complex is presented below.

The processes leading to the observed temperature dependence of the phosphorescence decay probably involve thermal equilibration of Trp excited states at the singlet level followed

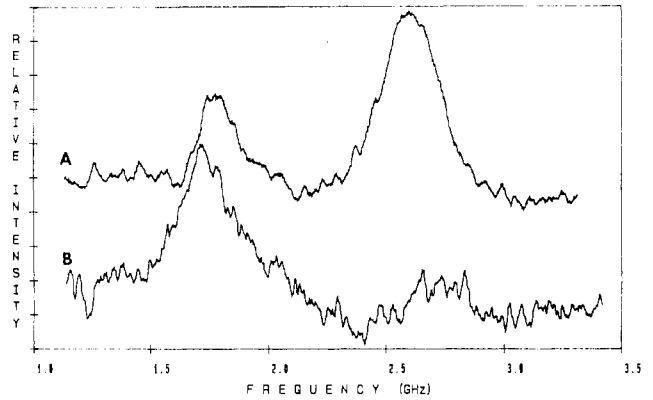

FIGURE 4: $|D| - |E|$ and $2|E|$ transitions of Trp in (A) pIP71a SSB (8.6×10^{-5} M) and (B) pIP71a SSB (8.6×10^{-5} M) complexed with poly(5-BrU) (1.35×10^{-3} M). Sweep rates are 58 (40 scans) and 310 MHz s^{-1} (400 scans) for (A) and (B), respectively. The temperature is 1.2 K, and the phosphorescence is monitored at (A) 412.2 and (B) 417 nm with 3-nm slits.

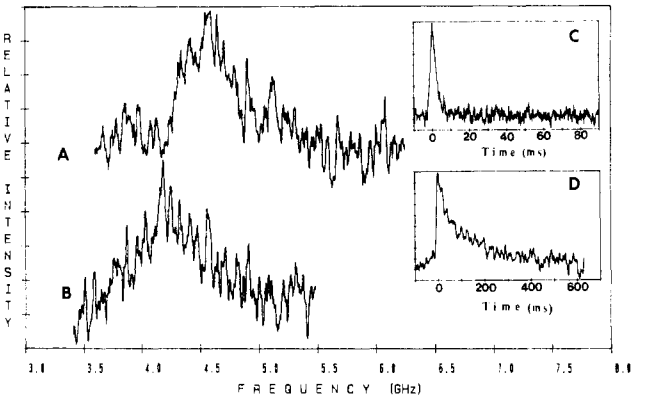

FIGURE 5: ODMR spectra at 1.2 K of heavy atom perturbed Trp in the $|D| + |E|$ region of (A) pIP71a SSB complexed with poly(5-HgU) and (B) pIP71a SSB complexed with poly(5-BrU). Sweep rates are 33 (4000 scans) and 2.86 GHz s^{-1} (2048 scans) for (A) and (B), respectively. (C) and (D) are fast-passage transients obtained at 1.2 K by sweeping the microwaves through the $|D| + |E|$ transition at 328 and 100 GHz s^{-1} for the pIP71a SSB–poly(5-HgU) complex and the pIP71a SSB–poly(5-BrU) complex, respectively. Phosphorescence is monitored at 413.6 nm for (A) and (C) and at 417 nm for (B) and (D), with 3-nm slit width.

by intersystem crossing to the local phosphorescent triplet state. Thermal equilibration of excited states at the triplet level is unlikely due to the limited range of triplet–triplet energy transfer (<5 Å) relative to singlet–singlet energy transfer (<40–50 Å).

ODMR Spectra. (A) pIP71a SSB and Its Complex with Poly(5-HgU). Figure 4A displays the $|D| - |E|$ and $2|E|$ ODMR signals of Trp residues in pIP71a SSB protein. The corrected peak frequencies together with the zero-field splitting parameters for the plasmid SSB proteins are presented in Table II. Comparison of the transition frequencies of these proteins with that of *Eco* SSB reveals no significant difference between them, in spite of the fact that Trp-135 in the C-terminal region of *Eco* SSB is missing in the other plasmid SSB proteins. Table II also includes the zero-field splitting parameters for the pIP71a SSB–poly(5-HgU) complex; these signals were obtained at microwave sweep rates 2 orders of magnitude faster than those for the free protein. This indicates that these signals must originate from a heavy atom perturbed triplet state since the long-lived triplet state of unperturbed Trp cannot respond to the rapid sweep conditions used. Comparison of the zero-field splitting parameters of pIP71a SSB–poly(5-HgU) complex with those of the *Eco* SSB–poly(5-HgU) complex (Table II) reveals a great similarity in the extent of heavy atom perturbation in each complex. The appearance of the normally absent $|D| + |E|$ signal (Figure 5A) provides strong evidence for the presence of a close-range interaction between the mercurated uridine bases and Trp residues. The fast-passage transient through this signal (Figure 5C) indicates that the perturbed Trp in this complex has an extremely short lifetime, similar to that observed earlier in the case of *Eco* SSB–poly(5-HgU) (Khamis et al., 1987). Analysis of this fast-passage response reveals a lifetime that is in the range of 2–5 ms for the more radiative sublevel. From the steric constraints and the extent of the external heavy atom effect, the mercurated uridine bases must stack with the indole moiety of Trp in order that the mercury atom is allowed to approach within van der Waals contact with the indole π-electrons from above or below the plane. An edge-on approach of a mercury atom to an aromatic molecule is known to produce a much less dramatic reduction of the sublevel lifetimes than is the case for an above-the-plane approach (Svejda et al., 1978). Steric possibilities other than stacking are ruled out since the Hg atom is covalently blocked with 2-mercaptoethanol. It is worth mentioning at this point that the close approach of the indole moiety of Trp to the nucleotide bases, leading to apposition of molecular orbitals (van der Waals contact), which has been referred to as stacking in this work, may be not equivalent to intercalation of these structures in the crystallographic sense.

(B) pIP71a SSB–Poly(5-BrU) Complex. The $|D| - |E|$ and $2|E|$ ODMR signals of the heavy atom perturbed Trp residue(s) in the pIP71a SSB–poly(5-BrU) complex are presented in Figure 4B. The peak frequencies together with the zero-field splitting parameters are found in Table II. It is noteworthy that the optimal sweep rate in obtaining these signals is 1 order of magnitude faster than those used for the free protein samples, which indicates the presence of Trp residues subjected to an external heavy atom effect. The appearance of the $|D| + |E|$ signal (Figure 5B) in this complex, which is diagnostic of a heavy atom effect, supports this finding. These results are similar to those observed in other SSB–poly(5-BrU) complexes (Khamis & Maki, 1986; Khamis et al., 1987). The fast-passage response through the $|D| + |E|$ region (Figure 5D) indicates the presence of a lifetime on the order of 100 ms for the more radiative sublevel. This finding provides strong support for our assignment of the ca. 500-ms component, observed in the decay profile of the pIP71a SSB–poly(5-BrU) complex and absent in both the free protein and the polynucleotide decay profiles, to a heavy atom perturbed Trp residue(s). Furthermore, the reduction of the $|D|$ values in this complex as compared with the free protein (Table II) indicates that these residues are involved in stacking interactions with the uridine bases, since aromatic stacking of Trp generally results in a reduction of its $|D|$ value (Co & Maki, 1978; Khamis et al., 1987). This is not surprising, since charge transfer in the triplet state, which is expected to accompany the stacking, results in an increase of z_{12}^2, where z_{12} is the interelectron distance of the triplet electron pair along the z (stacking) axis; a reduction of the $|D|$ value [$D \propto \langle (r_{12}^2 - 3z_{12}^2)/r_{12}^5 \rangle$] is the expected result, since D is positive for the Trp triplet state.

AM-PMDR of the pIP71a SSB–Poly(5-HgU) Complex. Figure 1C displays the AM-PMDR spectrum of the heavy atom perturbed Trp residue(s) in the pIP71a SSB–poly(5-HgU) complex and shows a poorly resolved, red-shifted 0,0-band (417 nm). This result, accomplished by amplitude modulating the microwave power in the $|D| + |E|$ signal region (nonobservable in the free protein) and sweeping the emission

monochromator through the phosphorescence region of the Trp chromophores employing lock-in detection at the modulating frequency, demonstrates that the apparent broadening of the phosphorescence spectrum upon binding poly(5-HgU) to pIP71a SSB is the result of an underlying heavy atom perturbed, red-shifted Trp component. Similar results were obtained for *Eco* SSB–poly(5-HgU) complexes (Khamis et al., 1987). It is interesting to compare the phosphorescence spectrum of the pIP71a SSB–poly(5-BrU) complex (Figure 2C) obtained at 4.2 K and of the *Eco* SSB–poly(5-BrU) complex at 4.2 K (Khamis et al., 1987) with the AM-PMDR spectra obtained upon binding poly(5-HgU) to each protein. There is a great similarity in each case between the AM-PMDR spectrum and the Br-perturbed Trp phosphorescence spectrum. This leads to the suggestion that the phosphorescence spectrum of the pIP71a SSB–poly(5-BrU) and of the *Eco* SSB–poly(5-BrU) complex, at 4.2 K, is due largely to heavy atom perturbed, stacked Trp residue(s). Phosphorescence decay measurements at 4.2 K (Figure 3) also support this suggestion.

Conclusions

The red-shifted phosphorescence spectra of the plasmid-encoded single-stranded DNA binding proteins pIP71a SSB, F SSB, and R64 SSB relative to that of *Eco* SSB indicate that Trp-135, which is missing in the former proteins, has a phosphorescence 0,0-band maximum that is <411 nm and contributes to a blue-shifted site in *Eco* SSB (Khamis et al., 1987). We were able to observe the external heavy atom effect [and hence stacking interactions between Trp residue(s) and heavy atom modified nucleotide bases] in pIP71a SSB complexes with poly(5-HgU) and poly(5-BrU). The resemblance of these effects to those observed for the complexes of *Eco* SSB with the above polynucleotides supports earlier models in which Trp-135 is not directly involved in the binding process (Williams et al., 1983; Khamis et al., 1987). Results presented here also indicate that not all of the remaining Trp residues (Trp-40, -54, and -88) undergo stacking interactions with the nucleotide bases, as is evident from the phosphorescence spectrum and lifetime measurements of the pIP71a SSB–poly(5-BrU) and –poly(5-HgU) complexes. Since pIP71a SSB and *Eco* SSB proteins have a high degree of amino acid sequence homology in their N-terminal domains, this sets an upper limit of two stacked Trp for the polynucleotide complexes of *Eco* SSB and pIP71a SSB. Although not presented as evidence for the occurrence of two functional Trp residues in *E. coli* SSB proteins, it is interesting to note that the estimated (random) occurrence of tryptophan in the primary structures of 207 unrelated proteins of known sequence is 1.1% (Klapper, 1977). In the primary sequence of *Eco* SSB (177 amino acid residues) the expected random occurrence of Trp would be two residues. Since *Eco* SSB contains four Trp residues, our estimate for the higher limit of two stacked, functional Trp residues is in accord with this statistical prediction. The presence of both functional and randomly occurring Trp causes some difficulty in assessing the role of the Trp residues of *Eco* SSB in stacking interactions. For instance, a 270-MHz ^{1}H NMR study concluded that *Eco* SSB binding does not include extensive stacking interactions between the nucleotide bases and the aromatic side chains of *Eco* SSB (Romer et al., 1984), although preliminary results of a 500-MHz study show perturbations of the aromatic region of the NMR spectrum upon oligonucleotide binding to *Eco* SSB (Chase & Williams, 1986).

In conclusion, we have provided evidence that the plasmid-encoded SSB proteins have similar interactions with single-stranded polynucleotides as does the wild-type *Eco* SSB, even though Trp-135 is absent. To identify which Trp residue(s) in *Eco* SSB undergoes (undergo) stacking interactions with polynucleotides, ODMR studies of *Eco* SSB proteins encoded by *ssb* genes carrying point mutations at the Trp positions are currently in progress in our laboratory.

Acknowledgments

We thank Mehdi Saghafi for expert technical assistance in carrying out the fluorometric titrations.

Registry No. Trp, 73-22-3; poly(dT), 25086-81-1.

References

Bandyopadhyay, P. K., & Wu, C. W. (1978) *Biochemistry 17*, 4078–4085.

Cha, T. A., & Maki, A. H. (1982) *Biochemistry 21*, 6586–6590.

Cha, T. A., & Maki, A. H. (1984a) *Biochim. Biophys. Acta 799*, 171–180.

Cha, T. A., & Maki, A. H. (1984b) *J. Biol. Chem. 259*, 1105–1109.

Chase, J. W. (1984) *BioEssays 1*, 218–222.

Chase, J. W., & Williams, K. R. (1986) *Annu. Rev. Biochem. 55*, 103–136.

Chase, J. W., Whittier, R. F., Auerbach, J., Sancar, A., & Rupp, W. D. (1980) *Nucleic Acids Res. 8*, 4215–4227.

Chase, J. W., Merrill, B. M., & Williams, K. R. (1983) *Proc. Natl. Acad. Sci. U.S.A. 80*, 5480–5484.

Chase, J. W., L'Italien, J. J., Murphy, J. B., Spicer, E. K., & Williams, K. R. (1984) *J. Biol. Chem. 259*, 805–814.

Co, T., & Maki, A. H. (1978) *Biochemistry 17*, 182–186.

Davis, J. M., & Maki, A. H. (1984) *Biochemistry 23*, 6249–6259.

Deubel, V., & Leng, M. (1974) *Biochimie 56*, 641–648.

Falaschi, A., Cobianchi, F., & Riva, S. (1980) *Trends Biochem. Sci. (Pers. Ed.) 5*, 154–157.

Ghosh, S., Weers, J. G., Petrin, M., & Maki, A. H. (1984) *Chem. Phys. Lett. 108*, 87–93.

Golub, E. I., & Low, K. B. (1983) *Proc. Natl. Acad. Sci. U.S.A. 80*, 1401–1405.

Golub, E. I., & Low, K. B. (1985) *J. Bacteriol. 162*, 235–241.

Hélène, C., & Maurizot, J. (1981) *CRC Crit. Rev. Biochem. 10*, 213–258.

Hélène, C., Toulmé, J.-J., & Montenay-Garestier, T. (1982) in *Topics in Nucleic Acid Structure* (Neidle, S., Ed.) Vol. 2, pp 229–285, Macmillan, New York.

Hershberger, M. V., Maki, A. H., & Galley, W. C. (1980) *Biochemistry 19*, 2204–2209.

Kasha, M. (1952) *J. Chem. Phys. 20*, 71–74.

Khamis, M. I., & Maki, A. H. (1986) *Biochemistry 25*, 5865–5872.

Khamis, M. I., Casas-Finet, J. R., & Maki, A. H. (1987) *J. Biol. Chem. 262*, 1725–1733.

Klapper, M. H. (1977) *Biochem. Biophys. Res. Commun. 78*, 1018–1024.

Kolodkin, A. L., Capage, M. A., Golub, E. I., & Low, K. B. (1983) *Proc. Natl. Acad. Sci. U.S.A. 80*, 4422–4426.

Köster, H., Hofer, B., Muller, H. H. G., & Kropelin, M. (1980) in *Biological Implications of Protein–Nucleic Acid Interactions* (Augustyniak, S., Ed.) pp 488–506, A. Mickiewicz University Press, Poznan.

Kowalczykowsky, S. C., Lonberg, N., Newport, J. W., & von Hippel, P. H. (1981) *Enzymes (3rd Ed.) 14a*, 373–444.

Krauss, G., Sindermann, H., Schomburg, U., & Maas, G. (1981) *Biochemistry 20*, 5346–5352.

Lieberman, H. B., & Witkin, E. M. (1983) *Mol. Gen. Genet. 190*, 92-100.
Lohman, T. M., & Overman, L. B. (1985) *J. Biol. Chem.* 260, 3594-3603.
Lohman, T. M., Overman, L. B., & Datta, S. (1986) *J. Mol. Biol. 187*, 603-615.
Maki, A. H., & Cha, T.-A. (1984) *Photochem. Photobiol., Proc. Int. Conf., 1983*, 1035-1055.
McConnell, B., & von Hippel, P. H. (1970) *J. Mol. Biol. 50*, 317-332.
Meyer, R. R., Glaser, J., & Kornberg, A. (1979) *Proc. Natl. Acad. Sci. U.S.A. 76*, 1702-1705.
Michelson, A. M., Pondon, J., & Grunberg-Manago, M. (1962) *Biochim. Biophys. Acta 55*, 529-540.
Molineux, I. J., Pauli, A., & Gefter, M. L. (1975) *Nucleic Acids Res. 2*, 1821-1837.
Olmsted, J., & El-Sayed, M. A. (1974) in *Creation and Detection of the Excited State* (Ware, W. R., Ed.) pp 1-62, Marcel Dekker, New York.
Purkey, R. M., & Galley, W. C. (1970) *Biochemistry 9*, 3569-3574.
Rahn, R. O., Yamane, T., Eisinger, J., Longworth, J. W., & Shulman, R. G. (1966) *J. Chem. Phys. 45*, 2947-2954.
Svejda, P., Maki, A. H., & Anderson, R. R. (1978) *J. Am. Chem. Soc. 100*, 7138-7145.
T'so, P. O. P., Rapaport, S. A., & Bollum, F. J. (1966) *Biochemistry 5*, 584-600.
Whittier, R. F., & Chase, J. W. (1983) *Mol. Gen. Genet. 190*, 101-111.
Williams, K. R., & Konigsberg, W. (1981) in *Gene Amplification and Analysis* (Chirikjian, J., & Papas, T., Eds.) Vol. 2, pp 475-508, Elsevier/North-Holland, New York.
Williams, K. R., Spicer, E. K., LoPresti, M. B., Guggenheimer, R. A., & Chase, J. W. (1983) *J. Biol. Chem. 258*, 3346-3355.
Winscom, C. J., & Maki, A. H. (1971) *Chem. Phys. Lett. 12*, 264-268.

Mechanism of Oxygen Activation by Tyrosine Hydroxylase†

Thomas A. Dix,‡,§ Donald M. Kuhn,‖ and Stephen J. Benkovic*,‡
Department of Chemistry, The Pennsylvania State University, University Park, Pennsylvania 16802, and Department of Psychiatry, Lafayette Clinic, Wayne State University, Detroit, Michigan 48207
Received September 12, 1986; Revised Manuscript Received January 29, 1987

ABSTRACT: The mechanism by which the tetrahydropterin-requiring enzyme tyrosine hydroxylase (TH) activates dioxygen for substrate hydroxylation was explored. TH contains one ferrous iron per subunit and catalyzes the conversion of its tetrahydropterin cofactor to a 4a-carbinolamine concomitant with substrate hydroxylation. These results are in accord with shared mechanisms of oxygen activation by TH and the more commonly studied tetrahydropterin-dependent enzyme phenylalanine hydroxylase (PAH) and strongly suggest that a peroxytetrahydropterin is the hydroxylating species generated during TH turnover. In addition, TH can also utilize H_2O_2 as a cofactor for substrate hydroxylation, a result not previously established for PAH. A detailed mechanism for the reaction is proposed. While the overall pattern of tetrahydropterin-dependent oxygen activation by TH and PAH is similar, the H_2O_2-dependent hydroxylation performed by TH provides an indication that subtle differences in the Fe ligand field exist between the two enzymes. The mechanistic ramifications of these results are briefly discussed.

The tetrahydrobiopterin (BPH_4)[1]-dependent mixed-function oxidase tyrosine hydroxylase (TH) catalyzes the formation of DOPA from tyrosine and serves as the control point in catecholamine biosynthesis (Kaufman & Kaufman, 1984). While long presumed to be related to (if not identical with) the more extensively studied tetrahydropterin-dependent enzyme phenylalanine hydroxylase (PAH), firm evidence addressing this assumption has only recently become available due to the extreme difficulty in purifying sufficient quantities of TH for biochemical analysis. It is established that, while the enzymes share a significant (48%) sequence homology (Ledley et al., 1985; Dahl & Mercer, 1986), cofactor requirements, and characteristics of cofactor utilization, important differences exist as to subunit molecular weights and the mechanisms by which they are regulated in vivo (Shiman, 1985; Kaufman & Kaufman, 1985). The key question, whether TH activates oxygen by the same mechanism as does PAH, has been mainly unexplored.

Scheme I

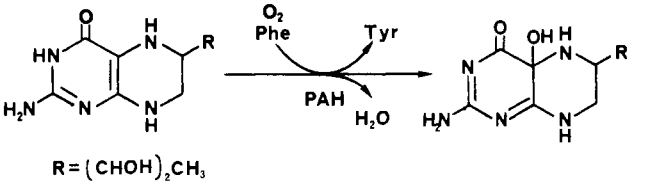

In this paper, we examine the nature of oxygen activation by TH using our previous results with PAH as a guide. During

† This work was supported by National Science Foundation Grant PCM 8103670 (to S.J.B.).
‡ The Pennsylvania State University.
§ National Institutes of Health postdoctoral fellow (GM09854). Present address: Department of Chemistry, The University of California, Irvine, CA 92717.
‖ Wayne State University.

[1] Abbreviations: BPH_4, L-*erythro*-tetrahydrobiopterin; TH, tyrosine hydroxylase; DOPA, L-3,4-dihydroxyphenylalanine; PAH, phenylalanine hydroxylase; 6-MPH_4, 6-methyltetrahydropterin; Tris, tris(hydroxymethyl)aminomethane; BPH_2, 7,8-dihydrobiopterin; EDTA, ethylenediaminetetraacetic acid; *m*-CPBA, *m*-chloroperoxybenzoic acid.

0006-2960/87/0426-3354$01.50/0